# Development and Characterization of Joining Techniques for Dispersion-Strengthened Alumina

*Active brazing technology proves successful in joining ceramic to ceramic and ceramic to steel*

BY E. LUGSCHEIDER, W. BÜRGER AND U. BROICH

ABSTRACT. The suitability of active brazing technology for joining TiC-strengthened alumina (ATC) to itself and to stainless steel is evaluated. The main emphasis is put on the investigation of the microstructural and mechanical properties of the active brazed joints. Furthermore, the electrical properties are investigated by determining the specific electrical resistance of active brazed $Al_2O_3$/TiC joints.

For fabrication of the joints two process technologies are applied: vacuum furnace brazing and induction brazing under shielding gas.

Four-point bend tests revealed that some of the vacuum-brazed ATC joints reach bending strengths comparable to those of bulk ATC. The induction brazing process is shown to be applicable when ATC has to be joined to metals, as in stainless steel for example. However, mechanically tough ATC-steel joints can only be fabricated when using very ductile filler metals, which are able to compensate thermally induced stresses by plastic deformation.

## Introduction

Titanium carbide-strengthened alumina (ATC) (70 wt-% $Al_2O_3$, 30 wt-% TiC) is a newly developed ceramic material with beneficial technological features. Besides excellent mechanical properties, the main characteristic of ATC is its electrical conductivity, which is comparable to that of graphite. The combination of excellent mechanical properties with good electrical conductivity offers interesting applications for ATC in mechanical and electrical engineering.

Some possible applications are slide and ignition contacts, power resistors and heating elements. In addition to these innovative applications, ATC is also suitable for conventional applications, such as wear-resistant components and cutting tools.

However, each application that is considered suitable for ATC requires an adequate joining technique that enables fabrication of mechanically tough, as well as corrosion-resistant and electrically conductive, joints. A joining process that is flexible enough to fulfill the variety of requirements is active brazing.

The high flexibility of active brazing technology is based on the possibility to apply various filler metals, which provide special properties to the joints. Within the present study, a variety of filler metals is investigated with regard to their suitability for brazing ATC to itself and to stainless steel. The investigations concentrate on the characterization of the joint microstructure and the determination of the mechanical and electrical properties. Vacuum brazing and induction brazing technology are evaluated for joining ATC to stainless steel.

*E. LUGSCHEIDER and U. BROICH are with Materials Science Institute at the Aachen University of Technology, Aachen, Germany. W. BÜRGER is with Hermsdorf Institute for Technical Ceramics, Hermsdorf, Germany.*

**KEY WORDS**

High-Performance Ceramics
Dispersion-Strengthened Oxides
Ceramic Brazing
High-Temp. Brazing
Active Brazing
Vacuum Furnace Brazing
Induction Brazing
Ceramic-Metal Joints
Four-point Bend Strength
Metallographic Analysis

## Materials and Experimental Procedure

### Materials

Dispersion-strengthened alumina (ATC) is a commercially available ceramic material fabricated by the Hermsdorf Institute of Technical Ceramics e.V. in Hermsdorf, Germany. The ceramic consists of two phases: alumina and titanium carbide. The mechanical and technological properties of ATC are strongly dependent on the amount of TiC. A favorite composition of ATC with regard to electrical conductivity and bending strength is at 70 wt-% $Al_2O_3$ and 30 wt-% TiC. The physical and technological properties of ATC with this favorite composition are given in Ref. 1.

Besides beneficial mechanical properties, which are partly superior to those of $Al_2O_3$ and SiC, the most favorable characteristic of ATC is its excellent electrical conductivity. The bulk material is fabricated in a three-step process: cold-isostatic pressing, sintering and hot-isostatic pressing. With this procedure, a microstructure with a theoretical density of

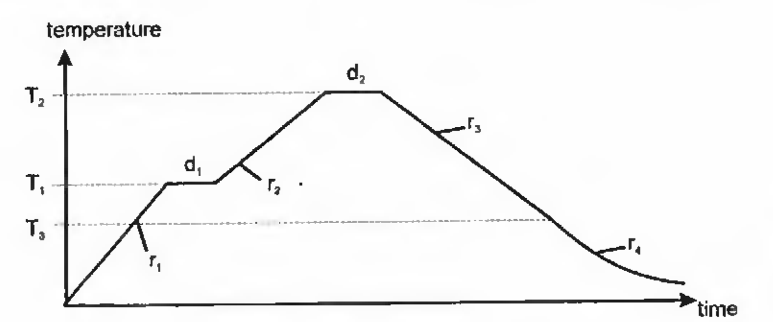


| | $r_1$ [K/min] | $T_1$ / | $d_1$ [min] | $r_2$ [K/min] | $T_2$ / | $d_2$ [min] | $r_3$ [K/min] | $T_3$ [°C] |
|---|---|---|---|---|---|---|---|---|
| **vac. braz.** | 15 | $T_{sol}$-50K | 10 | 10 | $T_{braze}$ | 5-30 | 15 | 500 |
| **ind. braz.** | 400 | $T_{braze}$-200K | 0 | 50 | $T_{braze}$ | 1-2 | / | / |

*Fig. 1 — Temperature-time run of the vacuum brazing and induction brazing processes.*

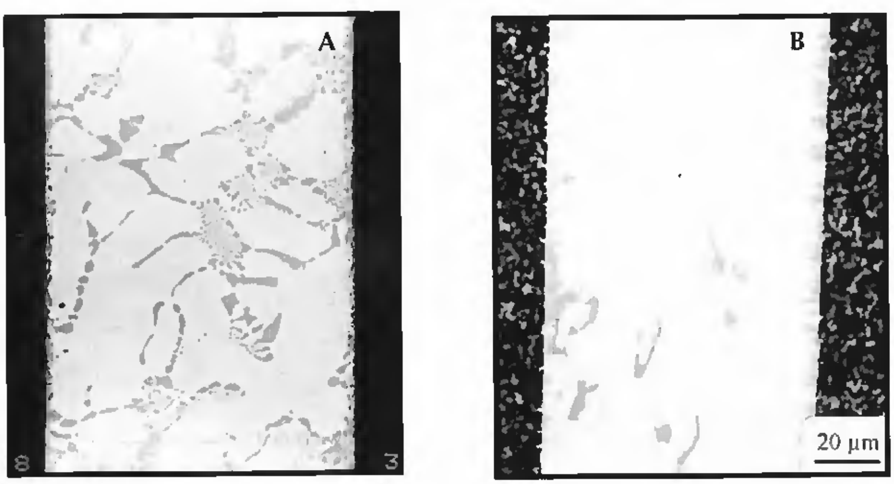


| Elements in reaction layer | Ti | O | Cu | Al |
|---|---|---|---|---|
| Element-fraction [at.%] | 29 | 56 | 13 | 2 |

*Fig. 2 —Microstructure of two vacuum brazed ATC joints. A — Filler metal: AgCuInTi, brazing parameters: 900°C/10 min; B — filler metal: CuSiAlTi, brazing parameters: 1050°C/10 min.*

99.5% can be achieved.

For brazing experiments, the surface of the ceramic was first ground and then cleaned in an ultrasonic bath filled with alcohol. The roughness of the surface after grinding was $R_z = 0.6$ µm.

The active filler metals that were used in the brazing experiments are given in Table 1. Filler metals No. 1–5 are commercially available alloys with titanium as a reactive agent. Filler metal No. 5 is an active solder characterized by very low melting temperatures and high ductility. The Au- and Pd-based filler metals are experimental alloys that have been developed for fabrication of temperature- and corrosion-resistant ceramic joints (Ref. 4). Therefore, the main feature of both filler metals is their high melting temperature, which requires very high brazing temperatures. For the brazing experiments, filler metal foils were used. The thickness of the foils generally was 100 µm; only the SnAgTi active solder foils had a thickness of 250 µm.

For the ATC-metal brazing experiments, the austenitic stainless steel X5 CrNi 18 9 (0.05 wt-%C, 18 wt-%Cr, 9 wt-%Ni) was chosen. The coefficient of thermal expansion (CTE), which is of major interest for the brazing process, is between 17 and $19 \cdot 10^{-6}$ 1/K, and thus is about twice as high as that of ATC (Ref. 5). Therefore, formation of thermally induced stresses can be expected when brazing ATC to this stainless steel.

#### Brazing Procedure

For the brazing experiments, two processes were used: vacuum furnace brazing and induction brazing under shielding gas. The induction brazing equipment consisted of a high-frequency generator with a maximum power supply of 3.0 kW and a frequency of 200 kHz, and a chamber in which a cylindrical inductor was located. Due to sufficient electrical conductivity of the ATC ceramic material, application of a susceptor was not necessary to heat up the samples. Brazing was done under argon atmosphere with a purity of 99.999%. During brazing, the argon pressure in the chamber was 1.15 bar. The brazing temperature was measured by a Ni-CrNi thermocouple, which was fixed in a 1.5-mm drill hole, located in the metal part, 4 mm below the brazing zone.

The geometry of the induction brazing samples was 3.5 x 4.5 x 30 mm. The samples were used for the metallograhic analysis, as well as for the four-point bend tests.

The temperature-time runs being applied within the brazing experiments in the vacuum furnace and the induction chamber, respectively, are given in Fig.1. The temperature-time run for the fabrication of the ATC-steel joints in the vacuum furnace was quite similar to that for the pure ceramic joints. Only the cooling rate was changed to a minor gradient, due to expansion mismatch of the bound materials. The vacuum pressure at brazing temperature was about $5 \cdot 10^{-5}$ mbar.

### Results and Discussion

#### Metallographic Analysis of Vacuum Brazed ATC-Joints

Figure 2 exhibits the microstructures of two ATC joints brazed in a vacuum furnace with AgCuInTi and CuSiAlTi, respectively. It can be seen that both filler metals have wetted the ATC ceramic. This is especially revealed by the existence of reaction layers, that have stabilized at the ceramic interfaces of both joints. In order to get some information about the composition of these reaction layers, EDX analysis was done at the AgCuInTi joint. The results of this analysis, which are also given in Fig. 2, reveal, that the reaction layers are titanium enriched and, moreover, predominantly contain oxygen and copper. This, however, leads to the conclusion that titanium has diffused to the ceramic interface in order to undergo chemical interactions with the alumina matrix of the ATC. It can be expected that during these titanium-alumina interactions titanium-oxide phases have been formed predominantly. This is also confirmed by a variety of authors, who have investigated the titanium-alumina reaction system quite deeply (Refs. 6–10).

Although the formation of reaction layers is necessary for wetting, from the technological point of view, formation of thick reaction layers is undesirable. The reason can be seen in the brittle character of the reaction layers. Thus, it is a major goal in brazing process optimization to prevent massive reaction-layer growth. As reaction-layer formation and growth are diffusion controlled processes, the brazing time is an adequate process parameter to control reaction-layer formation. Table 2 shows the influence of brazing time on the reaction-layer thickness of an AgCuInTi and CuSiAlTi joint, respectively. As the reaction layers are fairly irregular, the thickness values listed in Table 2 are mean values. As can be seen from the graph, for both joints, the reaction-layer thickness increases with rising brazing time. However, a reaction layer increase is much more evident for the AgCuInTi-joint.

The interface microstructure of a high-temperature brazed ATC-AuPdTi joint is shown in Fig. 3. In contrast to the AgCu- and Cu-based joints, no reaction-layer can be seen in the micrograph. To investigate the wetting mechanism of the Au-based filler metal, a titanium distribution analysis was done that is also presented in Fig. 3. Obviously, a very thin titanium-enriched layer has been formed at the ceramic interface, which most probably is the reaction layer that has provided wetting.

The fabrication of ATC joints with PdNiTi filler metal was quite difficult because of the bad wetting properties of the system. Figure 4 shows a micrograph of the joint interface. It can be seen that the interface between brazing zone and ATC is characterized by a 40–50-µm-thick decomposed area. Taking a closer look at

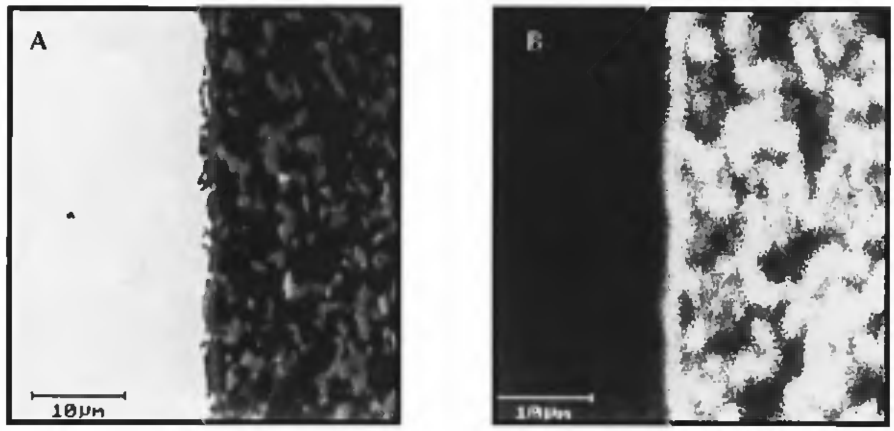


*Fig. 3 — Micrograph (A) and titanium distribution picture (B) of an ATC joint, brazed with AuPdTi. Brazing parameters: 1250°C/min.*

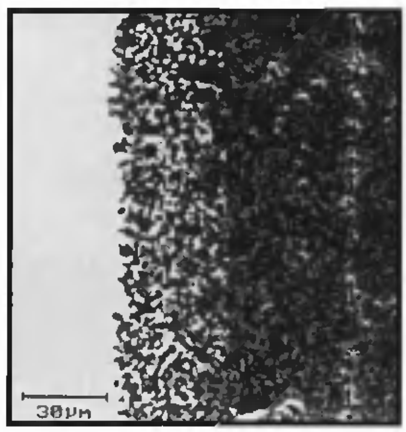


*Fig. 4 — Microstructure of a vacuum-brazed ATC joint. Filler metal: PdNiTi; brazing parameter: 1250°C/5 min.*

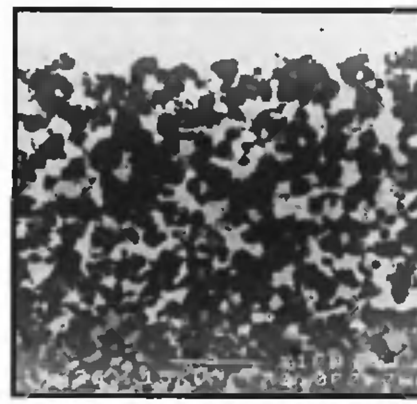

*Fig. 5 — Microstructure of the decomposed area of the vacuum-brazed ATC joint shown in Fig. 4. Filler metal: PdNiTi; brazing parameters: 1250°C/5 min.*

**Table 1 — Chemical Composition and Melting Temperatures of the Used Active Filler Metals (Refs. 2, 3)**

| Number | Filler Metal | Chemical Composition (wt-%) | $T_{sol}$ (°C) | $T_{liq}$ (°C) | $T_{braze}$ (°C) Vacuum/Induction |
|---|---|---|---|---|---|
| 1 | AgCuInTi | 72.5–19.5–5–3 | 730 | 760 | 900/900 |
| 2 | CuSiAlTi | 92.75–3–2–2.25 | 958 | 1024 | 1050/— |
| 3 | AgInTi | 98–1–1 | 950 | 960 | —/1150 |
| 4 | AgTi | 96–4 | 970 | 970 | —/1100 |
| 5 | SnAgTi | 86–10–4 | 221 | 300 | —/900 |
| 6 | AuPdTi | 90–8–2 | 1148 | 1205 | 1250/— |
| 7 | PdNiTi | 58–39–3 | 1224 | 1236 | 1250/— |

**Table 2 — Influence of Brazing Time on Reaction Layer Thickness of an AgCuInTi and CuSiAlTi Joint**

| Joint | ATC-AgCuInTi-ATC | | ATC-CuSiAlTi-ATC | |
|---|---|---|---|---|
| Brazing parameters | 900°C/10 min | 900°C/30 min | 1050°C/10 min | 1050°C/30 min |
| Reaction-layer thickness | 2.3 µm | 4.5 µm | 2.0 µm | 2.5 µm |

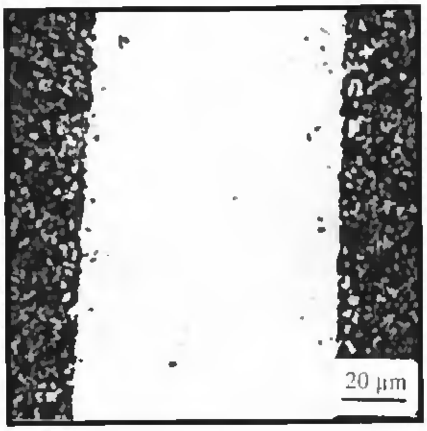


*Fig. 6 — Microstructure of a modified brazed joint. Filler metal: PdNiTi; brazing parameters: 1250°C/5 min, premetallized with AgCuInTi at 900°C/5 min.*

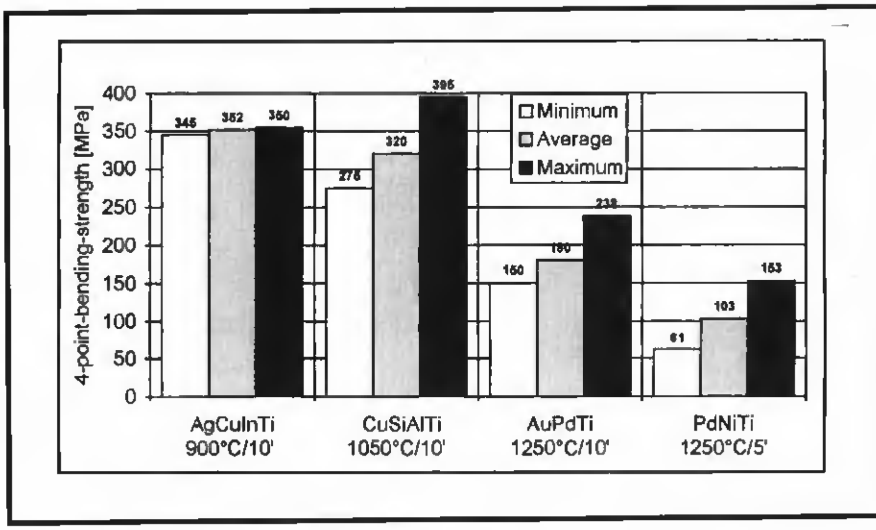


*Fig. 7 — Four-point bend strength of vacuum-brazed ATC-ATC joint.*

**Table 3 — Specific Electrical Resistance of Vacuum-Brazed ATC Joints**

| Joint | ATC | SnAgTi | CuSiAlTi | AgCuInTi | AuPdTi |
|---|---|---|---|---|---|
| Brazing parameters | as-received | 900°C/10 min | 1050°C/10 min | 900°C/10 min | 1250°C/10 min |
| Electrical resistance | 0.004 Ω·cm | 0.004 Ω·cm | 0.004 Ω·cm | 0.005 Ω·cm | 0.08 Ω·cm |

the decomposed area under high magnification (Fig. 5), it can be seen that the gray TiC phase has been decomposed, whereas the black $Al_2O_3$ particles are more or less unaffected. Obviously, the PdNi matrix system of the filler metal has strongly interacted with the TiC particles in the ATC during the high-temperature process.

In order to achieve sufficient wetting, a process modification was considered. The basic idea of this process modification was to metallize the ceramic before joining is done to provide a kind of sealing. Heretofore, a two-step joining process was applied. In the first heating process, the ceramic bound materials were metallized in a vacuum brazing process by using the reaction-layer-forming active filler metal AgCuInTi. The filler metal was applied by using a foil of 100-µm thickness. The aim of this premetallization was to induce the formation of a regular reaction layer. In a second step, the metallized surface was ground to achieve a plane surface. During grinding care must be taken that the reaction layer being formed during the premetallization process remains unaffected. As a consequence, a small layer of AgCu alloy remains on the surface of the ceramic sample. During the following high-temperature brazing process, the reaction layer works as a kind of sealing and protects the ceramic from massive decomposition by the molten PdNiTi alloy. The modified brazing procedure is derived from a patent described in Ref. 11. In Fig. 6, the microstructure of a PdNiTi joint brazed with the modified process can be seen. The ATC-bound material has successfully been prevented from decomposing during the high-temperature process, which can be attributed to the sealing function of the premetallization.

### Mechanical Properties of Vacuum-Brazed ATC Joints

For the four-point bend experiments, the brazed samples were tested in the as-brazed condition. For each of the conditions shown in Fig. 7, four to five specimens were used. The highest strength values are achieved by the AgCuInTi joints. With an average value of 350 MPa, the bending strength is even comparable to that of bulk ATC. This is also confirmed by the location of failure of the samples, which was 5–8 mm from the brazing zone within the bound material. The mechanical properties of the Cu-based joints are slightly poorer than those of the AgCu-based joints. The typical failure mechanism of Cu-based joints can be derived from Fig. 8. The structure of the fractured surface hints at thermally induced stresses in the ATC ceramic, due to expansion mismatch between ceramic and filler metal. It can be concluded that the mismatch stresses are much higher, when the Cu-based filler metals are used, due to comparatively lower ductility and higher solidus temperature of the filler metal. As the thermally induced stresses in the ceramic part are superposed by external forces during four-point bend testing, the bending strength of the joint strongly depends on the amount of thermally induced stresses. Due to the fact that the highest mismatch stresses can be found near the interface region in the ceramic part, failure of the joints normally start at the free surface of the ceramic quite near the brazing zone.

The bending strengths of the high-temperature brazed ATC joints are generally much lower. This is probably due to higher thermally induced stresses caused by the high solidus temperature of these filler metals. The comparatively lower bending strength of PdNiTi joints can be attributed to the lower ductility of PdNiTi compared to AuPdTi.

### Metallographic Analysis of Vacuum-Brazed ATC-Stainless Steel Joints

For fabrication of ATC-stainless steel joints, AgCuInTi, CuSiAlTi and SnAgTi filler metals were applied. Figure 9 shows the microstructures of the corresponding ATC-steel joints.

The brazing zone microstructure of the AgCuInTi joint is characterized by two reaction layers that have stabilized at the ceramic and steel interface, respectively, and a metallic brazing zone that consists of an Ag-rich matrix and embedded Cu crystals. The brazing zone does not contain large amounts of steel elements. The microhardness is about 160HV 0.005. The structure of the brazing zone can most probably be attributed to the reaction layer at the steel interface, which is an impediment for diffusion of steel elements into the brazing zone. A similar effect is reported by Schuster, *et al.* (Ref. 12), who found out that TiN, a reaction product formed during brazing of $Si_3N_4$, works as a diffusion barrier for Si.

The CuSiAlTi joint shows a completely different microstructure. The ceramic interface is characterized by the missing of a regular reaction layer, whereas a wide diffusion zone has formed at the steel interface. Element analysis revealed that this diffusion zone is enriched with silicon and titanium, which have diffused from the filler metal into the steel. As can be derived from the microhardness marks, the diffusion zone increased in microhardness.

The active-soldered ATC-steel joint is also characterized by the missing of a regular reaction layer at the ceramic interface. The structure of the steel interface, on the other hand, hints at massive interactions. Along the interface, several clusters of reaction products have concentrated. The metallic brazing zone is characterized by a very ductile Sn matrix, into which intermetallic Sn-Ti phases are embedded.

**Metallographic Analysis of Induction-Brazed ATC-Stainless Steel Joints**

Besides the AgCuInTi alloy, two more filler metals that have special suitability for induction brazing under inert gas were used: AgInTi and AgTi. Both filler metals are distinguished by very high ductility due to the large amount of silver (>95 wt-%). On the other hand, these alloys cannot be brazed under high-vacuum conditions due to massive evaporation of silver at brazing temperature. Figure 10 shows the microstructures of the induction brazed joints.

Concerning the AgCu-based joint (Fig. 10A), the brazing zone looks exactly the same as that of the corresponding vacuum brazed joint — Fig. 9A. This demonstrates that a brazing time of one minute is obviously sufficient for establishing chemical interactions between the active filler metal and the bound materials. However, the crack at the steel interface reveals that the level of thermally induced stresses in the joint is quite high.

Figure 10B and 10C shows the brazing zone microstructure of the Ag-based joints. In both joints, reaction layers have formed at the steel and ceramic interface. The main difference with regard to the microstructure can be seen in the thickness of these reaction layers. Due to the higher amount of the reactive agent in the AgTi alloy (4 wt-% Ti), the reaction layer of the AgTi joint is much thicker than that of the AgInTi joint (1 wt-% Ti).

**Mechanical Properties of Vacuum and Induction Brazed ATC-Stainless Steel Joints**

The four-point bend strengths of the vacuum-brazed ATC-steel joints are given in Fig. 11. First of all, it can be recognized that the strength values are generally lower than those of the corresponding ATC-ATC joints. The reason can be seen in a weakening of the joints, due to the large expansion mismatch of the bound materials. The weakening of the joints is characterized by the formation of thermally induced stresses in the ceramic part near the interface to the metallic brazing zone. The level of thermally induced stresses in the ceramic part is mainly affected by the solidus temperature and the properties of the component materials, especially thermal expansion coefficients and elastic modulii.

The Cu-based joints, for example, show the poorest mechanical strength because of the high solidus temperature and relatively low ductility of the filler metal compared to Ag- and AgCu-based filler metals. The high level of thermally induced stresses within this joint is especially confirmed by the fracture mecha-


*Fig. 8 — Fractured surface of a bending specimen brazed with CuSiAlTi at 1050°C/10 min.*

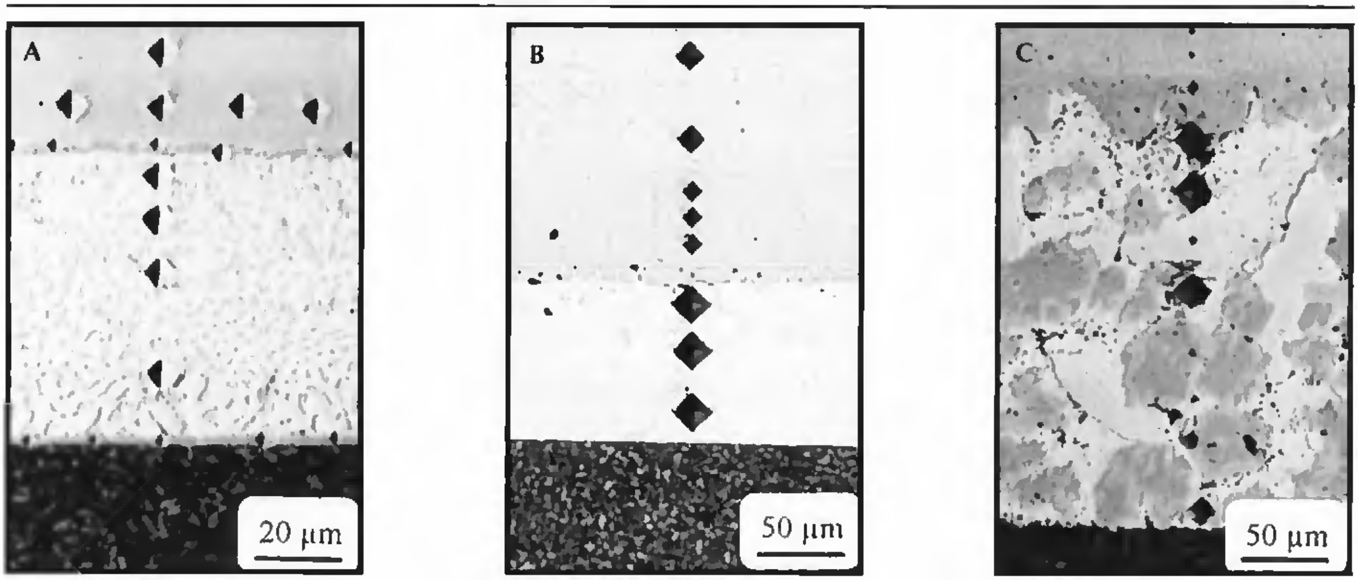


*Fig. 9 — Microstructures of three vacuum-brazed ATC-stainless steel joints. A — Filler metal AgCuInTi, brazing parameter 900°C/10 min; B — filler metal: CuSiAlTi, brazing parameter: 1050°C/10 min; C — filler metal: AgInTi, brazing parameter: 1150°C/2 min.*

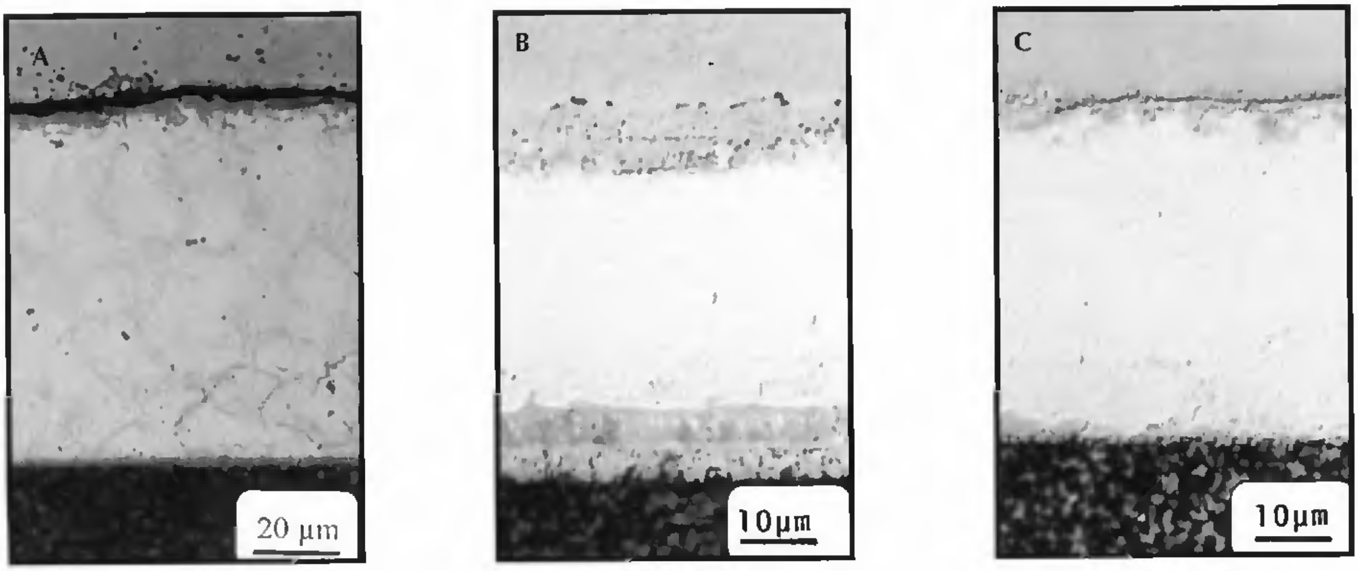


*Fig. 10 — Microstructures of three induction brazed ATC-stainless steel joints. A — Filler metal: AgCuInTi, brazing parameter: 900°C/1 min; B — filler metal: AgTi, brazing parameter: 1100°C/1 min; C — filler metal: AgInTi, brazing parameter: 1150°C/2 min.*

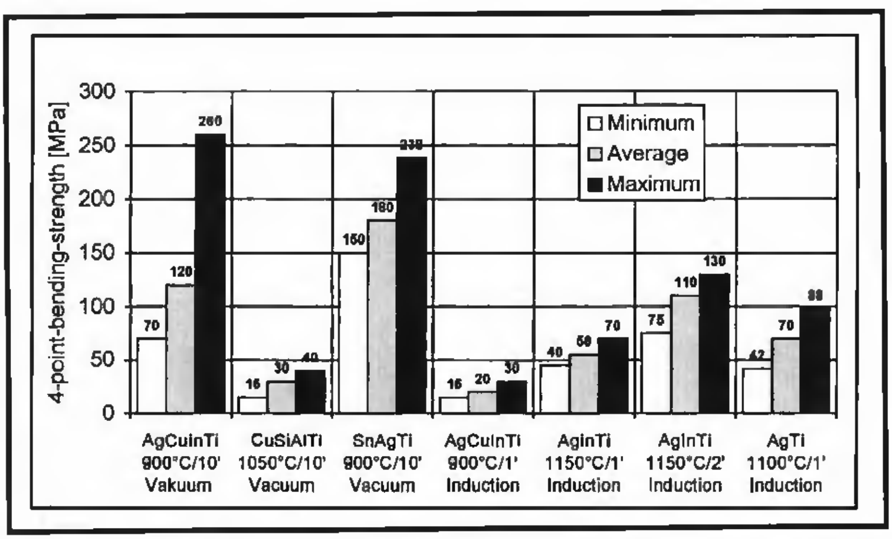


*Fig. 11 — Four-point bend strengths of vacuum- and induction-brazed ATC-stainless steel joints.*

nism. All joints failed in the ceramic bound material near the brazing zone.

The AgCuInTi joints clearly show higher bending strengths, which can be attributed to the lower solidus temperature. Nevertheless, the joints also failed within the ceramic part without exception.

The most beneficial strength properties are achieved by the active solder SnAgTi. In contrast to the other ATC-steel joints, the failure took place in the metallic brazing zone. This special failure mechanism of the active-soldered joints is due to the extraordinary low melting temperature and the very high ductility of the filler metal, which provide low mismatch stresses in the ceramic part.

The mechanical properties of the induction-brazed ATC-steel joints are also given in Fig. 11. Regarding the AgCuInTi-joints, it can be seen that the strength of the induction brazed samples is clearly below those of the vacuum brazed samples. Nevertheless, good mechanical strength can be achieved when applying the very ductile Ag-based filler metals. The AgInTi joints show excellent mechanical properties, although brazing time has a big influence on the strength. Those samples brazed with one minute brazing time show bad adhesion properties. The fractured surface of the brazed samples revealed that a major part of the ceramic surface has not been wetted by the filler metal, which might be due to the fact that a regular reaction layer has not been formed. When increasing brazing time to two minutes, the bending strength of the joints increases dramatically and the fracture mechanism is changed. All samples failed completely in the ceramic bound material near the brazing zone. Obviously, exceeding of brazing time leads to an improvement of wetting due to an extension of chemical interactions between filler metal and ceramic.

#### Electrical Properties of Active-Brazed ATC Joints

For investigation of the electrical properties of ATC joints, the specific electrical resistance was determined by measuring the voltage drop at a constant current. The results of these investigations are given in Table 3. It can be seen that the vast majority of the brazed joints have the same specific electrical resistance as bulk ATC. Consequently, neither the brazing zone nor the reaction layer affect the electrical conductivity.

The exceptionally poor conductivity of the AuPdTi joints is caused by an oxidation of the conducting TiC phase at the surface of the ceramic part during the high-temperature brazing process, as EDX analysis revealed. The oxidation of the TiC phase, however, leads to the formation of $TiO_2$ phases, which are electrically isolating.

## Summary and Conclusions

Active brazing is a suitable joining technique for ATC. This is confirmed by the beneficial electrical and mechanical properties of the active-brazed ATC joints. Those joints that have been brazed with AgCuInTi-filler metal reach bending strengths comparable to those of bulk ATC.

Besides joining ATC to itself, active brazing also allows fabrication of ATC-metal joints. However, mechanical properties are generally poorer than those of ATC-ATC joints. It was also shown that the induction brazing process is an interesting alternative to the vacuum furnace brazing technique when ATC has to be joined to steels. When using the very ductile Ag-based alloys AgTi and AgInTi, high quality joints can be fabricated by induction heating. Main advantages of the induction brazing process are short processing time, cheap equipment and low energy input into the parts.

*Acknowledgments*

The authors wish to express their gratitude to the Minister of Science and Research for financial support in the development of scientific research. Moreover, the authors wish to express their gratitude to Degussa Ltd. for providing the active filler metals used in this investigation.

*References*

1. Bürger, W. 1994. Elektrische Leitfähigkeit und Grenzflächeneigenschaften metallisierter $Al_2O_3$-TiC-Mischkeramik. *Keramische Zeitschrift,* 46(8): 47.

2. Prospect of Degussa Ltd., Hanau/Germany.

3. Prospect of GTE Wesgo Ltd., Belmont/USA.

4. Lugscheider, E., and Tillmann, W. 1992. Fügen von Keramik bei hohen Betriebstemperaturen. *Werkstoff und Innovation,* 5(5/6): 44.

5. N. N. Stahlschlüssel, Verlag Stahlschlüssel.

6. Santella, M. L., Horton, J. A., and Pak, J. J. 1990. Microstructure of alumina brazed with a silver-copper-titanium alloy. *Journal of the American Ceramic Society,* 73(6): 1785.

7. Moorhead, A. J., Henson, H. M., and Henson, I. J. 1988. *The Role of Interfacial Reactions on the Mechanical Properties of Ceramic Brazements.* Plenum Press, Vol. 21. p. 949.

8. Loehman, R. E., and Tomsia, A. P. 1988. Joining of Ceramics. *Ceramic Bulletin,* Vol. 67, p. 375.

9. Cho, H. C., and Yu, J. 1992. Effects of brazing temperature on the fracture toughness of $Al_2O_3$/AgCuTi joints. *Scripta Metallurgica et Materialia.* Vol.26. p. 797.

10. Crispin, R. M., and Nicholas, M. G. 1984. Reactive brazing of alumina to metals. *Brazing and Soldering,* No. 6., p. 3.

11. *Deutsche Patentanmeldung* P 41 05 596.9-45, Nr. 1006207, 22.02.1991.

12. Schuster, J. C., Weitzer, F., Bauer, J., and Nowotny, H. 1988. Joining of silicon nitride ceramics to metals: the phase diagram base. *Materials Science and Engineering,* A 105/106, p. 201.